Article:

Tian, Y., Gao, X., Liu, W. orcid.org/0000-0003-2968-2888 et al. (1 more author) (2022) Phase compensation based localization of mixed far-field and near-field sources. IEEE Wireless Communications Letters, 11 (3). pp. 598-601. ISSN 2162-2337

https://doi.org/10.1109/lwc.2021.3137488

Phase Compensation Based Localization of Mixed Far-Field and Near-Field Sources

Ye Tian, *Member, IEEE*, Xinyu Gao, Wei Liu, *Senior Member, IEEE*, and Hua Chen, *Member, IEEE*

***Abstract*—For mixed far-field (FF) and near-field (NF) source localization, most existing algorithms are developed for the scenario where the number of available data samples N is much larger than the number of sensors M. Different from these methods, this letter attempts to deal with the scenario where M is large and of the same order of magnitude as N. To obtain a satisfied performance in such a scenario, the phase compensation result of the spike covariance matrix is first utilized to construct a modified spectral function and successively realize the DOA estimation of FF sources. Then, we exploit the oblique projection operation to extract the NF sources. Finally, DOA and range estimation for NF sources is achieved via two one-dimensional (1-D) spectral searches, where the reconstructed manifold vector combining the phase compensation result is used. The effectiveness of the proposed algorithm is demonstrated by computer simulations.**

***Index Terms*—Source localization, far-field, near-field, phase compensation, modified spectral function.**

I. Introduction

MIXED far-field (FF) and near-field (NF) source localization is an important issue in array signal processing, and several types of solutions have been introduced in literature, such as the higher order statistic (HOS) based algorithms [1-4], the second-order statistics (SOS) based algorithms [5-7], the mixed-order statistics (MOS) based algorithms [8], [9] and the spatial differencing algorithm [10]. These algorithms can yield excellent performance, provided that the number of sensors M is small, whereas the number of data samples N is sufficiently large.

However, in some applications, the number of available data samples N is rather limited and of the same order as M, such as in massive MIMO/large-scale array systems [11], [12], or in scenarios where the signals are short-time stationary [13]. In this situation, the performance of existing algorithms mentioned above could degrade substantially, due to difficulty in estimating their statistics effectively [14]-[16].

To tackle this challenge, a novel mixed source localization algorithm is proposed in this letter, for scenarios where M is relatively large and comparable with the number of data samples N. Instead of applying the classical subspace based approach directly, the statistical analysis result obtained in the general asymptotic theory (GAT) for the case of $M, N \to \infty$ with $M/N = c \in (0, 1)$ is exploited for mixed source localization. In detail, the phase compensation result of the spike covariance matrix is first exploited to construct a modified spectral function, and 1-D search is then performed to obtain DOA estimation of FF sources; secondly, the contribution of FF sources is eliminated using the oblique projection operation and DOA estimation of NF sources is achieved by splitting the array manifold vector into two parts; finally, range estimation of NF sources is obtained after substituting each estimated NF DOA back into the modified 1-D spectral function.

Notations: Throughout this letter, boldface uppercase (lowercase) letters represent matrices (vectors). The superscripts $(\cdot)^T$ and $(\cdot)^H$ represent the transpose and conjugate transpose, respectively. $E\{\cdot\}$, $\mathrm{spec}(\cdot)$, $\mathrm{diag}\{\cdot\}$ and $\det[\cdot]$ denote statistical expectation, eigenvalues of a matrix, diagonalization and determinant, respectively. $\|\cdot\|$ stands for the Frobenius norm, $\langle \mathbf{a}, \mathbf{b} \rangle$ the dot product of $\mathbf{a}$ and $\mathbf{b}$, and $\mathbf{I}_M$ the $M \times M$ identify matrix. $\xrightarrow{a.s.}$ and $\xrightarrow{D}$ denote almost certain convergence and convergence in distribution, respectively. $\mathcal{N}(\cdot)$ indicates the normal distribution.

II. Signal Model

Suppose K narrowband signals (including K_1 FF sources and $K - K_1$ NF sources) impinge on a symmetric uniform linear array (SULA) with $M = 2L + 1$ sensors, where the distance d between adjacent sensors is equal to a quarter of the carrier wavelength λ. Let the center of array be the reference point, and then the output $\mathbf{x}(t)$ of the array can be modeled as

$$\mathbf{x}(t) = \mathbf{A}_F \mathbf{s}_F(t) + \mathbf{A}_N \mathbf{s}_N(t) + \mathbf{n}(t) = \mathbf{A}\mathbf{s}(t) + \mathbf{n}(t), \quad (1)$$

where $\mathbf{A} = [\mathbf{A}_F, \mathbf{A}_N]$, $\mathbf{s}(t) = [\mathbf{s}_F^T(t), \mathbf{s}_N^T(t)]^T$, and

$$\mathbf{A}_F = [\mathbf{a}(\theta_1, \infty), \cdots, \mathbf{a}(\theta_{K_1}, \infty)], \quad (2)$$

$$\mathbf{A}_N = [\mathbf{a}(\theta_{K_1+1}, r_{K_1+1}), \cdots, \mathbf{a}(\theta_K, r_K)], \quad (3)$$

$$\mathbf{a}(\theta_k, \infty) = [e^{-jL\varpi_k}, \ldots, 1, \ldots, e^{jL\varpi_k}], \quad (4)$$

$$\mathbf{a}(\theta_k, r_k) = [e^{-j(L\varpi_k - L^2\phi_k)}, \ldots, 1, \ldots, e^{j(L\varpi_k + L^2\phi_k)}], \quad (5)$$

$$\mathbf{s}_F(t) = [s_1(t), \ldots, s_{K_1}(t)]^T, \quad (6)$$

$$\mathbf{s}_N(t) = [s_{K_1+1}(t), \ldots, s_K]^T, \quad (7)$$

$$\mathbf{n}(t) = [n_{-L}(t), \ldots, n_{-1}(t), n_0(t), n_1(t), \ldots, n_L(t)]^T, \quad (8)$$

$\varpi_k = -0.5\pi \sin\theta_k, \phi_k = 0.25\pi d\cos^2\theta_k / r_k$, θ_k and r_k are DOA and range of the kth signal, respectively.

This work was supported by the National Natural Science Foundation of China (NSFC) under Grants 62001256 and 61601398.

Y. Tian and H. Chen are with the Faculty of Information Science and Engineering, Ningbo University, Ningbo 315211, China (e-mail: tianye1@nbu.edu.cn; dkchenhua0714@hotmail.com).

X. Gao is with the School of Information Science and Engineering, Yanshan University, Qinhuangdao 066004, China (e-mail: 13722513680@163.com).

W. Liu is with the Department of Electronic and Electrical Engineering, University of Sheffield, Sheffield S1 3JD, U.K. (e-mail: w.liu@sheffield.ac.uk).

Throughout this letter, we make the following hypotheses:

1) The signals are statistically independent, zero-mean narrowband stationary processes.
2) The noise is zero-mean, complex white Gaussian and independent of all signals.
3) The number of sources K is known a *priori* or can be estimated accurately by the LS-MDL criterion [17].

III. Proposed Algorithm

A. DOA Estimation Of FF Sources

Based on (1), the covariance matrix of the array output can be expressed as

$$\mathbf{R}_x = E\{\mathbf{x}(t)\mathbf{x}^H(t)\} = \mathbf{A}\mathbf{R_s}\mathbf{A}^H + \sigma_n^2\mathbf{I}_M, \tag{9}$$

whose finite sample estimate can be calculated by

$$\hat{\mathbf{R}}_x = \frac{1}{N}\sum_{t=1}^{N}\mathbf{x}(t)\mathbf{x}(t)^H = \sum_{i=1}^{M}\hat{\lambda}_i\hat{\mathbf{u}}_i\hat{\mathbf{u}}_i^H, \tag{10}$$

where σ_n^2 is the variance of noise, $\hat{\lambda}_i$ and $\hat{\mathbf{u}}_i$ are the eigenvalues in descending order and corresponding eigenvectors of $\hat{\mathbf{R}}_x$, respectively. Further define $\mathbf{A}\mathbf{R_s}\mathbf{A}^H = \mathbf{\Lambda}\mathbf{\Lambda}^H = \sum_{i=1}^{K}\alpha_i\mathbf{v}_i\mathbf{v}_i^H$, where α_i and $\mathbf{v}_i$ are the true eigenvalues and eigenvectors of $\mathbf{\Lambda}\mathbf{\Lambda}^H$, respectively. When the sampled covariance matrix $\hat{\mathbf{R}}_x$ is an unbiased estimator, the following relationship holds [18]

$$\begin{aligned}\mathrm{spec}(\mathbf{R}_x) &= (\alpha_1, \cdots, \alpha_K, \underbrace{0, \cdots, 0}_{1\times(M-K)}) + \sigma_n^2(\underbrace{1, \cdots, 1}_{1\times M}) \\ &= \sigma_n^2(\frac{\alpha_1}{\sigma_n^2}+1, \cdots, \frac{\alpha_K}{\sigma_n^2}+1, \underbrace{1, \cdots, 1}_{1\times(M-K)}) \\ &= (\hat{\lambda}_1, \cdots, \hat{\lambda}_M).\end{aligned} \tag{11}$$

Unfortunately, it has been demonstrated in literature [19] that when M and N both approach infinity at the same rate, Eq. (11) does not hold, which means that the direct application of $\hat{\lambda}_i$ and $\hat{\mathbf{u}}_i$ are not a good choice for our case. Nevertheless, according to the asymptotic analysis [19], $\mathbf{\Lambda}\mathbf{\Lambda}^H + \sigma^2\mathbf{I}_M$ can be described as a "spiked" covariance with "spiked" eigenvalues $\hat{\lambda}_1, \cdots, \hat{\lambda}_K$, which have the following convergence characteristics in the GAT framework

$$\left[\hat{\lambda}_k\right]_{k=1}^{K} \xrightarrow{a.s.} \begin{cases} \frac{(\sigma_n^2+\alpha_k)(\sigma_n^2 c+\alpha_k)}{\alpha_k}, & \alpha_k > \sigma_n^2\sqrt{c} \\ \sigma_n^2(1+\sqrt{c})^2, & otherwise. \end{cases} \tag{12}$$

Then, we can calculate the unbiased estimation of α_k as

$$\tilde{\alpha}_k = \frac{1}{2}\left\{\hat{\lambda}_k - \hat{\sigma}_n^2(1+c) + \sqrt{[\hat{\lambda}_k - \hat{\sigma}_n^2(1+c)]^2 - 4\hat{\sigma}_n^2 c}\right\}, \tag{13}$$

where $\hat{\sigma}_n^2 = \frac{1}{M-K}\sum_{i=K+1}^{M}\hat{\lambda}_i$ is the maximum likelihood estimator of σ_n^2, and it is also biased in our case. Next, we exploit the high-dimensional probabilistic theorem [18] to show how to obtain an unbiased estimation of noise variance with $\hat{\sigma}_n^2$ and $\tilde{\alpha}_k$.

Theorem 1: Consider covariance matrix $\mathbf{R}_x = \mathbf{\Lambda}\mathbf{\Lambda}^H + \sigma_n^2\mathbf{I}_M$. Assume that $M, N \to \infty$, $c = M/N \in (0,1)$, and the largest eigenvalue specified by α_k satisfies $\alpha_k > \sigma^2\sqrt{c}$, and then the following holds [18]

$$\frac{M-K}{\sigma_n^2\sqrt{2c}}(\hat{\sigma}_n^2 - \sigma_n^2) + b(\sigma_n^2) \xrightarrow{D} \mathcal{N}(0,1), \tag{14}$$

where $b(\sigma_n^2) = \sqrt{\frac{c}{2}}(K + \sigma_n^2\sum_{k=1}^{K}\frac{1}{\alpha_k})$.

This theorem shows that there is a negative bias between $\hat{\sigma}_n^2$ and σ_n^2. Therefore, we apply the following bias-corrected estimator $\tilde{\sigma}_n^2$ to remove such negative bias, i.e.,

$$\tilde{\sigma}_n^2 = \hat{\sigma}_n^2 + \frac{b(\hat{\sigma}_n^2)}{M-K}\hat{\sigma}_n^2\sqrt{2c}, \tag{15}$$

where $b(\hat{\sigma}_n^2) = \sqrt{\frac{c}{2}}\left(K + \hat{\sigma}_n^2\sum_{k=1}^{K}\frac{1}{\tilde{\alpha}_k}\right)$ depends on the spiked values $\tilde{\alpha}_k$.

Considering the phase transformation of eigenvectors associated with the K largest eigenvalues, we get [19]

$$\langle\hat{\mathbf{u}}_k, \mathbf{v}_k\rangle^2 \xrightarrow{a.s.} \begin{cases} \frac{\alpha_k^2 - \sigma_n^4 c}{\alpha_k(\alpha_k+\sigma_n^2 c)}, & \alpha_k \geq \sigma_n^2\sqrt{c} \\ 0, & otherwise, \end{cases} \tag{16}$$

which directly yields that $\mathbf{v}_k = \varphi_k^{-1}\hat{\mathbf{u}}_k$, where $k \in [1, K]$, and $\varphi_k = \langle\hat{\mathbf{u}}_k, \mathbf{v}_k\rangle$ can be interpreted as the phase transformation between $\hat{\mathbf{u}}_k$ and $\mathbf{v}_k$.

Subsequently, the following fact holds

$$\mathbf{U}_s\mathbf{U}_s^H = \sum_{k=1}^{K}\mathbf{v}_k\mathbf{v}_k^H = \sum_{k=1}^{K}(\tilde{\varphi}_k^2)^{-1}\hat{\mathbf{u}}_k\hat{\mathbf{u}}_k^H, \tag{17}$$

where $\tilde{\varphi}_k^2 = \frac{\tilde{\alpha}_k^2 - \tilde{\sigma}_n^4 c}{\tilde{\alpha}_k(\tilde{\alpha}_k+\tilde{\sigma}_n^2 c)}$.

Based on the phase compensation and subspace theory, we can derive the following modified spectral function as

$$\eta_F(\hat{\theta}) = \left[\mathbf{a}^H(\theta,\infty)(\mathbf{I}_M - \sum_{k=1}^{K}(\tilde{\varphi}_k^2)^{-1}\hat{\mathbf{u}}_k\hat{\mathbf{u}}_k^H)\mathbf{a}(\theta,\infty)\right]^{-1}. \tag{18}$$

Consequently, the DOAs $\{\hat{\theta}_1, \cdots, \hat{\theta}_{K_1}\}$ of FF sources can be estimated by finding K_1 peaks of the above modified spectral function.

B. DOA Estimation of NF Sources

With the estimated DOAs of FF sources, we reconstruct its corresponding array manifold matrix as

$$\hat{\mathbf{A}}_F = [\mathbf{a}_F(\hat{\theta}_1), \cdots, \mathbf{a}_F(\hat{\theta}_{K_1})]. \tag{19}$$

Let $\mathbf{E}_{(\mathbf{A}_F\mathbf{A}_N)}$ be an oblique projection matrix with range space $\mathbf{A}_F$ and null space $\mathbf{A}_N$. For a large number of sensors, it has been proven that the following convergence holds [20]

$$\|\mathbf{E}_{(\mathbf{A}_F\mathbf{A}_N)} - \frac{1}{M}\mathbf{A}_F\mathbf{A}_F^H\| \xrightarrow{M\to\infty} 0, \tag{20}$$

which means that $\mathbf{E}_{(\mathbf{A}_F\mathbf{A}_N)}$ can be calculated by

$$\mathbf{E}_{(\mathbf{A}_F\mathbf{A}_N)} = \frac{1}{M}\hat{\mathbf{A}}_F\hat{\mathbf{A}}_F^H, \tag{21}$$

provided that M is large.

Subsequently, by applying the oblique projection operation, the signal component associated with NF sources is given by

$$\begin{aligned}\bar{\mathbf{x}}(t) &= (\mathbf{I}_M - \mathbf{E}_{(\mathbf{A}_F\mathbf{A}_N)})\mathbf{x}(t)\\ &= \mathbf{A}_N\mathbf{S}_N(t) + (\mathbf{I}_M - \mathbf{E}_{(\mathbf{A}_F\mathbf{A}_N)})\mathbf{n}(t),\end{aligned} \tag{22}$$

whose finite sample estimate is $\hat{\mathbf{R}}_N = \frac{1}{N}\sum_{t=1}^{N}\bar{\mathbf{x}}(t)\bar{\mathbf{x}}^H(t)$.

Performing the eigenvalue decomposition (EVD) on $\hat{\mathbf{R}}_N$ yields

$$\hat{\mathbf{R}}_N = \hat{\mathbf{E}}_S\hat{\mathbf{\Delta}}_S\hat{\mathbf{E}}_S^H + \hat{\mathbf{E}}_N\hat{\mathbf{\Delta}}_N\hat{\mathbf{E}}_N^H, \tag{23}$$

where $\hat{\mathbf{E}}_S = [\hat{\mathbf{e}}_1, \ldots, \hat{\mathbf{e}}_{K-K_1}]$ and $\hat{\mathbf{E}}_N = [\hat{\mathbf{e}}_{K-K_1+1}, \ldots, \hat{\mathbf{e}}_M]$ denote the $M \times (K - K_1)$-dimensional signal subspace and the $M \times (M - K + K_1)$-dimensional noise subspace, which correspond to the $K - K_1$ largest eigenvalues $\hat{\mathbf{\Delta}}_S = \mathrm{diag}\{[\hat{\delta}_1, \ldots, \hat{\delta}_{K-K_1}]\}$ and the left $M - K + K_1$ small eigenvalues $\hat{\mathbf{\Delta}}_N = \mathrm{diag}\{[\hat{\delta}_{K-K_1+1}, \ldots, \hat{\delta}_M]\}$, respectively.

Applying the same phase compensation scheme as (17), we can obtain the unbiased estimation of eigenvectors of NF sources, which satisfies

$$\mathbf{E}_S\mathbf{E}_S^H = \sum_{k=1}^{K-K_1}(\tilde{\phi}_k^2)^{-1}\hat{\mathbf{e}}_k\hat{\mathbf{e}}_k^H, \tag{24}$$

where $\tilde{\phi}_k$ is the phase transformation between the estimated value $\hat{\mathbf{e}}_k$ and true value $\mathbf{e}_k$.

In order to realize NF source localization efficiently, we divide the array manifold vector $\mathbf{a}_N(\theta_k, r_k)$ into two parts, where the first part only contains the DOA information and the other part contains both DOA and range information, i.e.,

$$\mathbf{a}_N(\theta_k, r_k) = \mathbf{V}(\theta_k)\mathbf{b}(\theta_k, r_k), \tag{25}$$

where $\mathbf{b}(\theta_k, r_k) = [e^{jL^2\phi_k}, \ldots, e^{jl^2\phi_k}, \ldots, 1]^T$, and

$$\mathbf{V}(\theta_k) = \begin{bmatrix} e^{-jL\varpi_k} & \cdots & 0 & \cdots & 0\\ \vdots & \ddots & \vdots & \cdots & \vdots\\ 0 & \cdots & e^{-jl\varpi_k} & \cdots & \vdots\\ \vdots & \cdots & \vdots & \ddots & \vdots\\ 0 & \cdots & 0 & 0 & 1\\ \vdots & \cdots & \vdots & \iddots & \vdots\\ 0 & \cdots & e^{jl\varpi_k} & \cdots & \vdots\\ \vdots & \iddots & \vdots & \cdots & \vdots\\ e^{jL\varpi_k} & \cdots & 0 & \cdots & 0 \end{bmatrix}. \tag{26}$$

Following the orthogonality property between array manifold vector and noise subspace, we have

$$\begin{aligned}&\mathbf{a}_N^H(\theta_k, r_k)\mathbf{E}_N\mathbf{E}_N^H\mathbf{a}_N(\theta_k, r_k)\\ &\quad= \mathbf{b}^H(\theta_k, r_k)\mathbf{V}^H(\theta_k)\mathbf{E}_N\mathbf{E}_N^H\mathbf{V}(\theta_k)\mathbf{b}(\theta_k, r_k)\\ &\quad= \mathbf{b}^H(\theta_k, r_k)\mathbf{P}(\theta)\mathbf{b}(\theta_k, r_k) = 0,\end{aligned} \tag{27}$$

where $\mathbf{P}(\theta) = \mathbf{V}^H(\theta_k)(\mathbf{I}_M - \mathbf{E}_S\mathbf{E}_S^H)\mathbf{V}(\theta_k)$.

Obviously, $\mathbf{a}_N^H(\theta_k, r_k)\mathbf{E}_N\mathbf{E}_N^H\mathbf{a}_N(\theta_k, r_k)$ will be zero if and only if $\mathbf{P}(\theta)$ is singular. In other words, the DOAs $\{\tilde{\theta}_{K_1+1}, \cdots, \tilde{\theta}_K\}$ of NF sources can be estimated by finding $K - K_1$ peaks of the following spectral function

$$\eta_N(\tilde{\theta}) = \{\det[\mathbf{V}^H(\theta_k)(\mathbf{I}_M - \sum_{k=1}^{K-K_1}(\tilde{\phi}_k^2)^{-1}\hat{\mathbf{e}}_k\hat{\mathbf{e}}_k^H)\mathbf{V}(\theta_k)]\}^{-1}. \tag{28}$$

C. Range Estimation of NF Sources

By substituting $\tilde{\theta}_k$ into the NF array manifold vector $\mathbf{a}_N(\theta_k, r_k)$ $\{k = K_1 + 1, \cdots, K\}$, the range estimation $\tilde{r}_k$ of NF sources can be finally obtained by the following 1-D spectral function

$$\eta_N(r_k) = [\mathbf{a}^H(\tilde{\theta}_k, r)(\mathbf{I}_M - \sum_{k=1}^{K}(\tilde{\varphi}_k^2)^{-1}\hat{\mathbf{u}}_k\hat{\mathbf{u}}_k^H)\mathbf{a}(\tilde{\theta}_k, r)]^{-1}, \tag{29}$$

where $\tilde{\theta}_k$ and $\tilde{r}_k$ are automatically paired.

IV. Numerical Simulations

In this section, the performance of the proposed algorithm is evaluated and also compared with those of the SOS-based oblique projection algorithm [6], the spatial differencing algorithm [10], and the Cramér-Rao bound (CRB). The additive noise is white Gaussian with variance $\sigma_n^2 = 1$. Two FF sources located at $(10°, \infty)$, $(12°, \infty)$ and two NF sources located at $(30°, 2\lambda)$ and $(50°, 2\lambda)$ impinge on an SULA with M sensors. The number of samples is fixed at $N = 80$, and all the sources are BPSK-modulated with equal power. The root mean square error (RMSE) of DOA and range estimation obtained from the average results of 1000 independent Monte-Carlo simulations is employed to evaluate the performance.

In the first simulation, RMSE curves of DOA and range estimation versus SNR are shown in Figs. 1 and 2, respectively. The number of sensors is set to $M = 61$ and SNR is varied from -5 dB to 25 dB. It can be seen that the proposed algorithm has outperformed all other algorithms for both DOA and range estimations, and its RMSEs are closer to the related CRBs. Meanwhile, it can been further observed that the RMSE of FF sources of different algorithms become the same in high SNR regions, this is because the two closely-spaced FF sources can be well separated under such a circumstance.

In the second simulation, we further assess the performance of different algorithms with different number of sensors. The SNR is set to 0 dB, and M varies from 31 to 71 at a step of 10. The result is shown in Figs. 3 and 4, from which we can see that the RMSEs of all algorithms decrease monotonically with the number of sensors M. Again, the proposed algorithm has achieved the best performance for the whole sensor number range. In particular, it can also be seen that the more sensors we have, the closer the RMSE of the proposed algorithm is to CRB, which implies that the proposed algorithm is more suitable for large-scale array scenarios. Moreover, due to the use of the same FF estimator for the oblique projection and the spatial differencing algorithms, we can see that they have identical performance for FF DOA estimation.

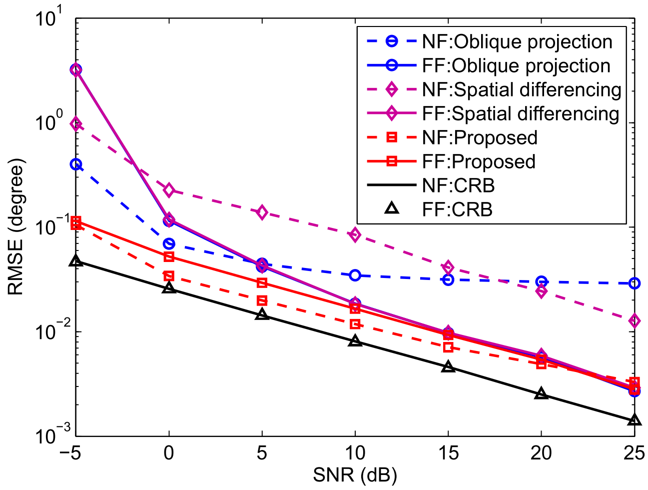

Fig. 1. RMSEs of DOA estimations for two FF and two NF sources versus SNR, with $M = 61$, $N = 80$.

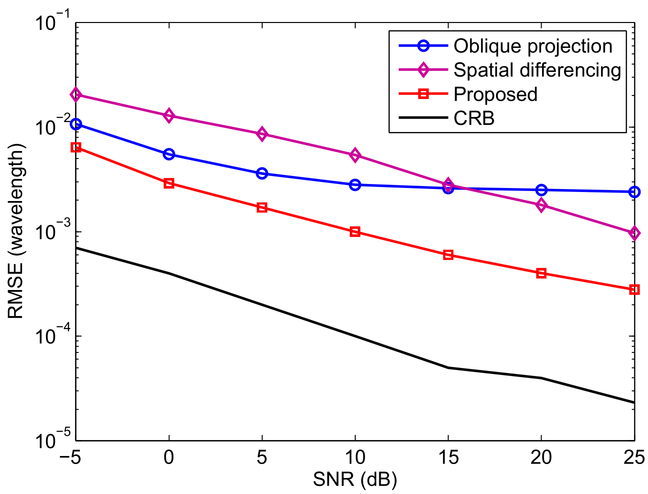

Fig. 2. RMSEs of range estimations for two FF and two NF sources versus SNR, with $M = 61$, $N = 80$.

V. Conclusion

In this letter, a novel localization algorithm for mixed FF and NF sources has been proposed from the GAT perspective when the number of data samples available is comparable with the number of sensors. Based on the property of the spike covariance matrix, three modified 1-D spectrum functions utilizing the phase compensation result are successively constructed. Compared with existing algorithms, an improved performance can be achieved by the proposed solution, as verified by numerical simulations.

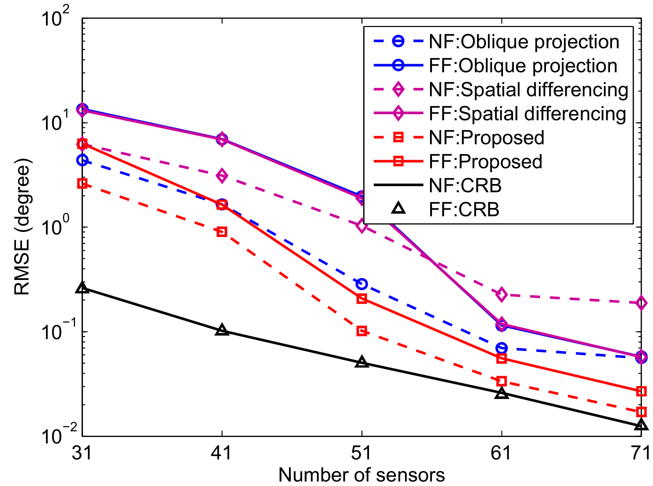

Fig. 3. RMSEs of DOA estimations for two FF and two NF sources versus number of sensors, with $N = 80$, SNR=0 dB.

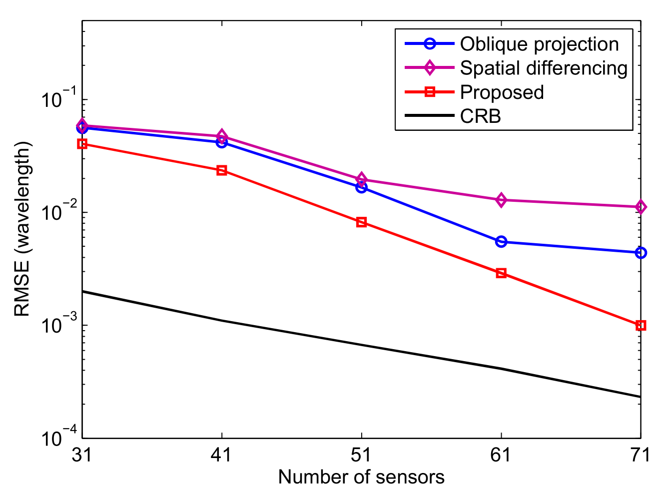

Fig. 4. RMSEs of range estimations for two FF and two NF sources versus number of sensors, with $N = 80$, SNR=0 dB.

References

[1] Z. Zheng, M. Fu, W. Wang, and H. C. So, "Mixed far-field and near-field source localization based on subarray cross-cumulant," *Signal Process.* vol. 150, pp. 51-56, 2018.

[2] H. Ma, H. Tao, and J. Xie, "Mixed far-field and near-field source localization using a linear tripole array," *IEEE Wireless Commun. Lett.*, vol. 9, no. 6 pp. 889-892, Jun. 2020.

[3] Z. Zheng, M. Fu, W. Wang, and H. C. So, "Symmetric displaced coprime array configurations for mixed near-and far-field source localization," *IEEE Trans. Antennas Propag.*, vol. 69, no. 1, pp.465-477, Jan. 2021.

[4] X. Wu and J. Yan, "3-D mixed far-field and near-field sources localization with cross array," *IEEE Trans. Veh. Technol.*, vol. 69, no. 6, pp. 6833-6837, Jun. 2020.

[5] X. Wu and J. Yan, "A second-order statistics-based mixed sources localization method with symmetric sparse arrays," *IEEE Commun. Lett.*, vol. 24, no. 8 pp. 1695-1699, Aug. 2020.

[6] J. He, M. N. S. Swamy, and M. O. Ahmad, "Efficient application of MUSIC algorithm under the coexistence of far-field and near-field sources," *IEEE Trans. Signal. Process.*, vol. 60, no. 4, pp.2066-2070. Apr. 2012.

[7] H. Chen, W. P. Zhu, et al., "RARE-based localization for mixed near-field and far-field rectilinear sources," *Digital Signal Process.*, vol. 85, pp. 54-61, Feb. 2019.

[8] J. He, L. Li, T. Shu, and T. K. Truong, "Mixed near-field and far-field source localization based on exact spatial propagation geometry, *IEEE Trans. Veh. Technol.*, vol. 70, no. 4, pp. 3540-3551, Apr. 2021.

[9] Z. Zheng, M. Fu, W.-Q. Wang, S. Zhang, and Y. Liao, "Localization of mixed near-field and far-field sources using symmetric double-nested arrays," *IEEE Trans. Antennas Propag.*, 2019, vol. 67, no. 11, pp. 7059-7070, Nov. 2019.

[10] G. Liu and X. Sun, "Spatial differencing method for mixed far-field and

near-field sources localization," *IEEE Signal Process. Lett.*, vol. 21, no. 11, pp. 1331-1335, Nov. 2014.

[11] S. Fortunati, F. Gini and M. S. Greco, "Massive MIMO radar for target detection," *IEEE Trans. Signal. Process.*, vol. 68, pp. 859-871, 2020.

[12] Y. Tian, W. Liu, H. Xu, S. Liu and Z. Dong, "2-D DOA estimation of incoherently distributed sources considering gain-phase perturbations in massive MIMO systems," *IEEE Trans. Wireless Commun.*, 2021, to be published. doi: 10.1109/TWC.2021.3102483.

[13] P. Vallet and Philippe Loubaton, "Toeplitz rectification and DOA estimation with music," in *Proc. IEEE Int. Conf. Acoust., Speech Signal Process.*, May 2014, pp. 2237-2241.

[14] R. Couillet, F. Pascal, and J. W. Silverstein, "Robust estimation of covariance matrices in the large dimensional regime," *IEEE Trans. Inform. Theory*, vol. 60, no. 11, pp. 7269-7278, Nov, 2014.

[15] Y. Liu, X. Sun, and S. Zhao, "A covariance matrix shrinkage method with Toeplitz rectified target for DOA estimation under the uniform linear array," *AEU-Int. Electron. Commun.*, vol. 81, pp. 50-55, 2017.

[16] Y. Tian, Y. Qin, Z. Dong, and H. Xu, "DOA estimation of coherently distributed sources in massive MIMO systems with unknown mutual coupling," *Digital Signal Process.*, vol. 111, pp. 102987, 2021.

[17] L. Huang and H. C. So, "Source enumeration via MDL criterion based on linear shrinkage estimation of noise subspace covariance matrix," *IEEE Trans. Signal. Process.*, vol. 61, no. 19, pp. 4806-4821, 2013.

[18] D. Passemier, Z. Li, and J. Yao, "On estimation of the noise variance in high-dimensional probabilistic principal component analysis," *J. Roy Stat Soc B. Met.*, vol. 79, no. 1, pp. 51-67, Jan. 2017.

[19] F. Benaych-Georges and R. Nadakuditi, "The eigenvalues and eigenvectors of finite, low rank perturbations of large random matrices," *Adv. Math*, vol. 227, no. 1, pp. 494-521, 2011.

[20] R. Boyer and G. Bouleux, "Oblique projections for Direction-Of-Arrival Estimation with Prior Knowledge," *IEEE Trans. Signal. Process*, vol.56, no. 4, pp. 1374-1387, Mar. 2008.